Strain Difference in Photoreceptor Cell Death After Retinal Detachment in Mice

Hidetaka Matsumoto, Keiko Kataoka, Pavlina Tsoka, Kip M. Connor, Joan W. Miller, and Demetrios G. Vavvas

Retina Service, Angiogenesis Laboratory, Massachusetts Eye and Ear Infirmary, Department of Ophthalmology, Harvard Medical School, Boston, Massachusetts, United States

Correspondence: Demetrios G. Vavvas, Massachusetts Eye and Ear Infirmary, 243 Charles Street, Boston, MA 02114;
Vavvas@meei.harvard.edu.

Submitted: February 24, 2014
Accepted: May 14, 2014

Citation: Matsumoto H, Kataoka K, Tsoka P, Connor KM, Miller JW, Vavvas DG. Strain difference in photoreceptor cell death after retinal detachment in mice. *Invest Ophthalmol Vis Sci*. 2014;55:4165–4174. DOI:10.1167/iovs.14-14238

Purpose. To evaluate the potential for mouse genetic background to effect photoreceptor cell death in response to experimental retinal detachment (RD).

Methods. Retinal detachment was induced in three inbred mouse strains (C57BL/6, BALB/c, and B6129SF2) by subretinal injection of sodium hyaluronate. A time course of photoreceptor cell death was assessed by TUNEL assay. Total photoreceptor cell death was analyzed through comparing the outer nuclear layer (ONL)/inner nuclear layer (INL) ratio 7 days post RD. Western blot analysis or quantitative real-time PCR (qPCR) were performed to assess cell death signaling, expression of endogenous neurotrophin, and levels of apoptosis inhibitors 24 hours after RD. Inflammatory cytokine secretion and inflammatory cell infiltration were quantified by ELISA and immunostaining, respectively.

Results. The peak of photoreceptor cell death after RD was at 24 hours in all strains. Photoreceptor cell death as well as monocyte chemoattractant protein 1 and interleukin 6 secretion at 24 hours after RD was the highest in BALB/c, followed in order of magnitude by C57BL/6 and B6129SF2. Conversely, nerve growth factor expression and ONL/INL ratio were the lowest in BALB/c. Apoptosis signaling was higher in C57BL/6, whereas necroptosis signaling was higher in C57BL/6 and BALB/c. Autophagic signaling was higher in BALB/c. X-linked inhibitor of apoptosis (XIAP) and survivin protein levels were lower in C57BL/6 and BALB/c, respectively. Macrophage/microglia infiltration was higher in C57BL/6 and BALB/c at 24 hours after RD.

Conclusions. Photoreceptor cell death after RD was significantly different among the three strains, suggesting the presence of genetic factors that affect photoreceptor cell death after RD.

Keywords: retinal detachment, retinal degeneration, photoreceptor death, cell death signaling, neurotrophins

Retinal detachment (RD) causes photoreceptor cell death and leads to visual decline; RD is involved in various retinal disorders, including rhegmatogenous RD,[1] AMD,[2] diabetic retinopathy,[3] and retinopathy of prematurity.[4] Therapeutic strategies for these diseases have been improved; however, visual acuity is not always restored after successful treatments due to the induction of photoreceptor cell death after RD. The model of RD is a powerful tool to study the mechanism by which photoreceptor cell death in the detached retina occurs and seek candidates for therapeutic target.[5–27] Specifically, the mouse model of RD allows investigators to take advantage of the genetic manipulation possible in mice.

It has been reported that apoptosis plays a critical role in photoreceptor cell death after RD.[6–8,10,14,17,24,25] Apoptosis occurs in either caspase-dependent or caspase-independent pathways. The former is regulated by the cascade of caspase family members, while the latter is mediated by soluble mitochondrial intermembrane proteins such as apoptosis-inducing factor (AIF).[28] We previously reported that necrosis is another pathway to induce photoreceptor cell death after RD, although its frequency is approximately one-half that of apoptosis.[25] Necrosis has been classically considered to be an accidental unregulated form of cell death, but recent studies demonstrated that the execution of necrotic cell death can be controlled.[29–32] This regulated necrosis pathway is called 'necroptosis' and is primarily regulated by the receptor-interacting protein (RIP) kinase.[33] More recently, autophagy activation was reported to occur in photoreceptor cells after RD.[26,27] It is characterized by the sequestration of cytoplasmic material within autophagosomes for degradation by lysosomes.[34] Microtubule-associated protein light chain 3 (LC3), an essential component of the autophagosome complex, is regarded as a marker for autophagy.[35]

It has been known that there are racial differences in the prevalence of some human ocular diseases including AMD,[36] glaucoma,[37] and Behçet disease.[38] Likewise, mouse genetic background has been reported to affect the biological reactions of the eye, such as light-induced photoreceptor cell death,[39] optic nerve crush induced ganglion cell death,[40] angiogenesis,[41] lymphangiogenesis,[42] etc. These reports lead us to surmise that genetic background might affect photoreceptor cell death after RD. To date, there is a lack of data on the possible difference in RD-induced photoreceptor cell death observed in inbred mouse strains.

In this study, we investigated the strain difference in photoreceptor cell death after induction of experimental RD using three inbred mouse strains: C57BL/6, BALB/c, and B6129SF2. C57BL/6 and BALB/c are the most widely used inbred strains. B6129SF2 mice are used as approximate controls for genetically engineered strains that were generated with 129-derived embryonic stem cells and maintained on a mixed B6; 129 background. We assessed photoreceptor cell death after RD by measuring TUNEL-positive cell density in the outer nuclear layer (ONL) and outer/inner nuclear layer (ONL/INL) ratio of the retina. We also assessed regulators and markers of apoptosis, necrosis, autophagy, neurotrophin, and inflammation, which have all both shown to contribute to neuronal death and/or survival. Our results showed significant differences among the three strains in levels of photoreceptor cell death, cell death signaling, neurotrophin expression, inhibitor of apoptosis (IAP) proteins, and inflammatory response after RD.

Methods

Animals

All animal experiments followed the guidelines of the ARVO Statement for the Use of Animals in Ophthalmic and Vision Research and were approved by the Animal Care Committee of the Massachusetts Eye and Ear Infirmary. C57BL/6 and BALB/c mice were purchased from Charles River Laboratories, Inc. (Wilmington, MA, USA). B6129SF2 mice were purchased from Jackson Laboratories (Bar Harbor, ME, USA). Each strain showed normal phenotype (Supplementary Fig. S1). Mice were fed standard laboratory chow and allowed free access to water in an air-conditioned room with a 12-hour light/12-hour dark cycle. All mice were used at postnatal 8 ± 1 weeks.

Creation of Retinal Detachment

We modified a previously reported method for creating bullous and persistent RDs.[43] Briefly, mice were anesthetized with an intraperitoneal injection of a mixture of 60 mg/kg ketamine and 6 mg/kg xylazine, and pupils were dilated with topical phenylephrine (5%) and tropicamide (0.5%). The temporal conjunctiva at the posterior limbus was incised and detached from the sclera. A 30-gauge needle (BD, Franklin Lakes, NJ, USA) was used with the bevel pointed up to create a sclerotomy 1 mm posterior to the limbus. A scleral tunnel was created, followed by scleral penetration into the choroid, which makes a self-sealing scleral wound. A corneal puncture was made with a 30-gauge needle to lower intraocular pressure. A 34-gauge needle connected to a 10-μL syringe (NanoFil 10-μL syringe; World Precision Instruments, Inc., Sarasota, FL, USA), was inserted into the subretinal space with the bevel pointed down. Then, 4 μL of 1% sodium hyaluronate (Provisc; Alcon, Fort Worth, TX, USA) was injected gently, detaching approximately 60% of the temporal-nasal neurosensory retina from the underlying RPE. Finally, cyanoacrylate surgical glue (Webglue; Patterson Veterinary, Devens, MA, USA) was applied to the scleral wound, and the conjunctiva was reattached to the original position. Eyes with subretinal hemorrhage were excluded from analysis.

TUNEL

The eyes with RD were enucleated and embedded in OCT compound (Tissue-Tek; Sakura Finetec, Torrance, CA, USA). Serial sections in the sagittal plane were cut at 10-μm thickness on a cryostat (CM1850; Leica, Heidelberg, Nussloch, Germany) at −20°C and prepared for staining. We performed TUNEL assays according to the manufacturer's protocol (ApoTag Fluorescein In Situ Apoptosis Detection Kit; Millipore, Billerica, MA, USA). Finally, sections were counterstained with TO-PRO-3. Cells that were TUNEL-positive were counted in the ONL, containing the photoreceptor cell bodies. The area of ONL was also measured by ImageJ software (http://imagej.nih.gov/ij/; provided in the public domain by the National Institutes of Health, Bethesda, MD, USA), and TUNEL-positive cell density in the ONL was calculated. Our preliminary experiments revealed that the center of RD had less variability of TUNEL-positive cell density (data not shown), so we used the sections around 1000 μm from the injection site. The average TUNEL-positive cell density at two parts of the retina (see Matsumoto et al.[44]) was calculated as the representative TUNEL-positive photoreceptor cell density of the section. Then, the average of the TUNEL-positive photoreceptor cell densities from three sections was determined as the representative TUNEL-positive photoreceptor cell density of the eye. Photographs were taken by confocal microscopy using a ×40 lens (HCX APOL; Leica Camera, Inc., Allendale, NJ, USA).

Evaluation of ONL/INL Ratio

The ONL and INL areas of the detached retina were measured by ImageJ software (National Institutes of Health), and ONL/INL ratio was calculated. Areas of abnormal retinal morphology were excluded so that uniform unbiased measurements could be obtained.

Western Blot Analysis

Retinas from experimental eyes with RD and control eyes without RD were dissected from the RPE-choroid. Total retinal lysate was used to evaluate the level of cleaved caspase 3, RIP3, and p-TrkA. Nuclear extraction was performed according to the manufacturer's protocol (Nuclear Extract Kit; Active Motif North America, Carlsbad, CA, USA) to assess AIF protein levels. Samples were electrophoresed on 4% to 12% or 12% Bis-Tris gel (NuPAGE; Invitrogen, Camarillo, CA, USA) and transferred onto polyvinylidene difluoride membranes (0.45-μm pores; Millipore Corp., Billerica, MA, USA). After blocking with 3% nonfat dried milk, the membranes were incubated overnight with primary antibody (cleaved caspace 3, AIF, phospho-TrkA, LC3, VDAC, β-actin, β-tubulin: 1:1000 (Cell Signaling, Danvers, MA, USA); TBP: 1:1000 (Abcam, Cambridge, UK); RIP3: 1:10,000 (Sigma-Aldrich, St. Louis, MO, USA). The blotted membranes were then incubated for 30 minutes at room temperature with HRP-labeled anti-rabbit secondary antibody. Immunoreactive bands were visualized by ECL and detected by a commercial imaging system (ChemiDoc MP; Hercules, CA, USA).

Measurement of mRNA Expression by Quantitative Real-Time PCR (qPCR)

Whole retina was used for qPCR. Total RNA was harvested using an RNA kit (RNeasy Kit; Qiagen, Valencia, CA, USA). cDNA was generated with Oligo-dT primer (Invitrogen) and Superscript II (Invitrogen) according to the manufacturer's instructions. Quantitative PCR was carried out using NGF (Mm00443039_m1) and β-actin (Mm00607939_s1) TaqMan gene expression assays (Applied Biosystems, Foster City, CA, USA). The housekeeping gene β-actin was used as an internal reference. Quantitative expression data were acquired and analyzed with a Step One Plus real-time PCR system (Applied Biosystems) using the ΔΔ Ct method.

Investigative Ophthalmology & Visual Science

ELISA for Monocyte Chemoattractant Protein 1 and Interleukin 6

The levels of monocyte chemoattractant protein (MCP)-1 and IL-6 were determined with mouse MCP-1 (R&D Systems, Inc., Minneapolis, MN, USA) and IL-6 (R&D Systems, Inc.) ELISA kits, according to the manufacturer's protocol.

Immunohistochemistry

Sections were fixed in acetone for 5 minutes, blocked in 2% skim milk for 20 minutes, and incubated with rat anti-CD11b antibody (1:50; BD Biosciences, San Jose, CA, USA) or rabbit anti-glial fibrillary acidic protein (GFAP) antibody (1:100; Dako, Carpinteria, CA, USA) at 4°C overnight. AlexaFluor 488–conjugated goat anti-rat or anti-rabbit IgG was used as a secondary antibody and incubated at room temperature for 30 minutes. Finally, sections were counterstained with TO-PRO-3.

Statistical Analysis

The results are expressed as the mean ± SE. Multiple-group comparison was performed by one-way ANOVA followed by Tukey-Kramer adjustments for all statistical analyses in the study. The significance level was set at $P < 0.05$ (* in figures) and $P < 0.01$ (** in figures). Statistical analysis was performed using graphing software (Prism version 5; GraphPad Software, Inc., La Jolla, CA, USA).

Results

Strain Difference in RD-Induced Photoreceptor Cell Death

To evaluate the photoreceptor cell death after RD in C57BL/6, BALB/c, and B6129SF2 mouse strains, we investigated a time course of photoreceptor cell death after induction of RD through TUNEL assessment. We analyzed TUNEL-positive cell density in the ONL at 12, 24, 48, 72, 120, and 168 hours after RD (Figs. 1A, 1B). In all three strains, TUNEL-positive cells peaked at day 1 after RD. TUNEL-positive cell density was significantly higher in BALB/c (2782 ± 165 cells/mm^2), followed in order by C57BL/6 (1663 ± 249 cells/mm^2) and B6129SF2 (814 ± 107 cells/mm^2; $^{**}P < 0.01$ each). However, at an earlier time point (12 hours), C57BL/6 was higher than BALB/c and B6129SF2 (825 ± 132 cells/mm^2 versus 311 ± 78 cells/mm^2 and 334 ± 64 cells/mm^2 respectively; $^{*}P < 0.05$ each). After day 1, there were no significant differences among the three strains (Fig. 1A). Other retinal layers displayed no TUNEL-positive cells after RD.

The significant strain difference in photoreceptor cell death was reflected in the ONL/INL ratio (Fig. 1C). The strain with the least TUNEL-positive cells (B6129SF2) showed the highest ONL/INL ratio (1.67 ± 0.06), followed in order by C57BL/6 (1.57 ± 0.03) and BALB/c (1.39 ± 0.04) ($^{*}P < 0.05$ for B6129SF2 versus BALB/c).

Strain Difference in Cell Death Signaling After RD

To compare the cell death signaling after RD among the three strains, we assessed cleaved caspase-3, AIF, RIP3, and LC3 II/I ratio at 24 hours after RD by Western blot (Fig. 2).

Caspase-3 is one of the effector caspases that are activated by cleavage and mediate apoptotic cell death. Cleaved caspase-3 was significantly higher in C57BL/6 (100%) than BALB/c (57%) and B6129SF2 (60%) ($^{*}P < 0.05$ each; Fig. 2A). Apoptosis-inducing factor is one of the intra-mitochondrial molecules that mediate caspase independent apoptosis; during apoptosis, they are released through the outer mitochondrial membrane and translocate into the nucleus.[8,28,45] Nuclear AIF was highest in C57BL/6, followed in order by BALB/c and B6129SF2 ($^{*}P < 0.05$ for C57BL/6 vs B6129SF2; Fig. 2B, Supplementary Fig. S2).

Another form of regulated cell death is RIP kinase-mediated necrosis. Holler and colleagues[29] discovered that RIP1 kinase is a key molecule that induces necrotic cell death mediated by FAS receptor. Receptor-interacting protein 3 was reported to be a key regulator of RIP1 kinase phosphorylation and necrotic signaling.[46] Moreover, we and other groups have shown RIP kinases to be significant players in photoreceptor cell death in RD.[25,47] Receptor-interacting protein 3 was significantly higher in C57BL/6 (100%) and BALB/c (97%) than B6129SF2 (59%) ($^{*}P < 0.01$ each; Fig. 2C).

Autophagy can contribute to cell survival or cell death. During the formation of autophagosomes, LC3 (LC3-I) is lipidated, and this LC3-phospholipid conjugate (LC3-II) is localized on autophagosomes.[35,48] The LC3 II/I ratio is regarded as a marker for autophagy, and was significantly higher in BALB/c (0.70) than C57BL/6 (0.46) and B6129SF2 (0.50; $^{*}P < 0.05$ each; Fig. 2D).

Strain Difference in Neurotrophin Expression After RD

Cell death is governed not only by cell death signaling but also by prosurvival pathways. Neurotrophin is essential in survival of neurons, and nerve growth factor (NGF) is the prototype for the neurotrophin family of polypeptides.[49] Nerve growth factor and its high-affinity tyrosine kinase receptor TrkA are confirmed to express in the retina.[50–56] Moreover, intravitreal injection of exogenous NGF has been reported to protect retinal cells from apoptosis in experimental RD.[57] In the current study, we evaluated *NGF* mRNA expression levels by qPCR at 24 hours after RD. BALB/c, which showed the most photoreceptor cell death, expressed significantly less *NGF* mRNA (47%) than C57BL/6 (100%) and B6129SF2 (126%; $^{**}P < 0.01$ each; Fig. 3A).

Nerve growth factor activates TrkA receptor tyrosine kinases through receptor dimerization, followed by autophosphorylation and resultant intracellular signaling.[58] Thus, we next evaluated phosphorylated TrkA protein levels by Western blot at 24 hours after RD to assess the binding between NGF and TrkA in the retina. Consistent with *NGF* mRNA levels, BALB/c displayed significantly less phosphorylated TrkA protein levels (69%) than C57BL/6 (100%) and B6129SF2 (106%; $^{*}P < 0.05$ each; Fig. 3B).

Strain Difference in Levels of IAP Proteins After RD

The IAP family proteins function as intrinsic regulators of the caspase cascade.[59] Thus, to further investigate the prosurvival pathways in the retina, we next evaluated levels of IAP proteins by Western blot at 24 hours after RD.

X-linked IAP (XIAP) binds active caspases and promotes the ubiquitination and degradation of active caspases. However, under the severe cellular stress, XIAP will undergo autoubiquitination and degrade, which allows unrestricted caspase activation.[59] Recently, XIAP gene therapy was reported to rescue photoreceptor cell death in an RD model.[60] In the current study, XIAP levels were decreased after RD in all strains, and significantly lower in C57BL/6 (64%) than BALB/c (84%) and B6129SF2 (87%; $^{*}P < 0.05$ each; Fig. 4A). These results are consistent with cleaved caspase-3 levels in each strain.

Survivin is also one of the IAP proteins and known for its association with cell cycle progression.[61] It has been reported

Investigative Ophthalmology & Visual Science

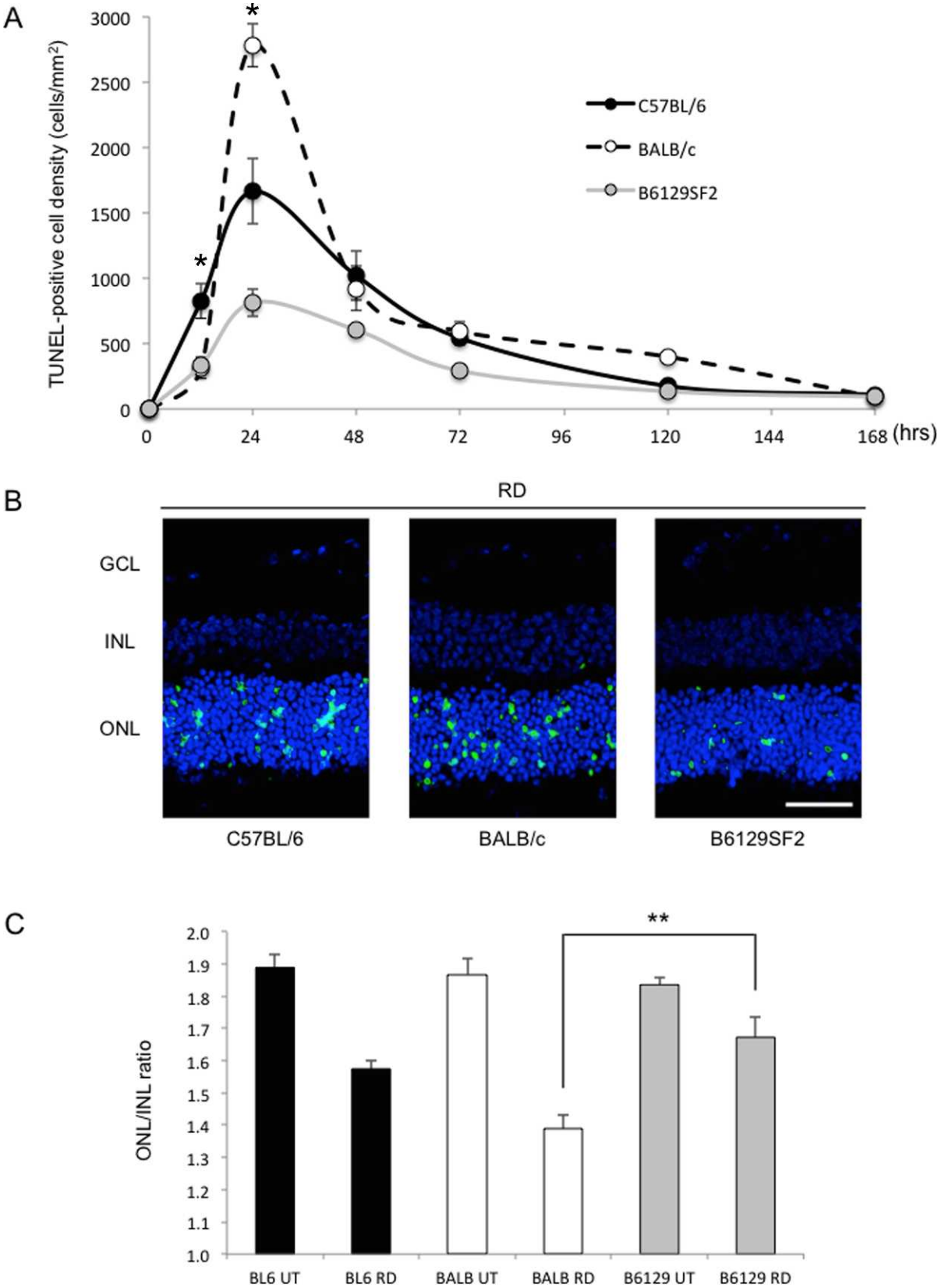

Figure 1. Difference in photoreceptor cell death induced by RD. (**A**) Time course of TUNEL-positive cell density in the ONL ($n = 6$ each group and time point). At 12 hours after RD, TUNEL-positive cell density was significantly higher in C57BL/6 than BALB/c or B6129SF2 (*$P < 0.05$ each). At 24 hours after RD, it was highest in BALB/c, followed in order by C57BL/6 and B6129SF2. There was a significant difference between each pair of strains (**$P < 0.01$ each). (**B**) TUNEL (*green*) and TO-PRO-3 (*blue*) staining at 24 hours after RD. (**C**) Ratio of ONL/INL before and 7 days after RD ($n = 6$ each). At day 7, ONL/INL ratio was highest in B6129SF2, followed in order by C57BL/6 and BALB/c. There was a significant difference between B6129SF2 and BALB/c (*$P < 0.05$). *Scale bar*: 50 μm. The graphs show mean ± SEM. GCL, ganglion cell layer; UT, untreated.

Investigative Ophthalmology & Visual Science

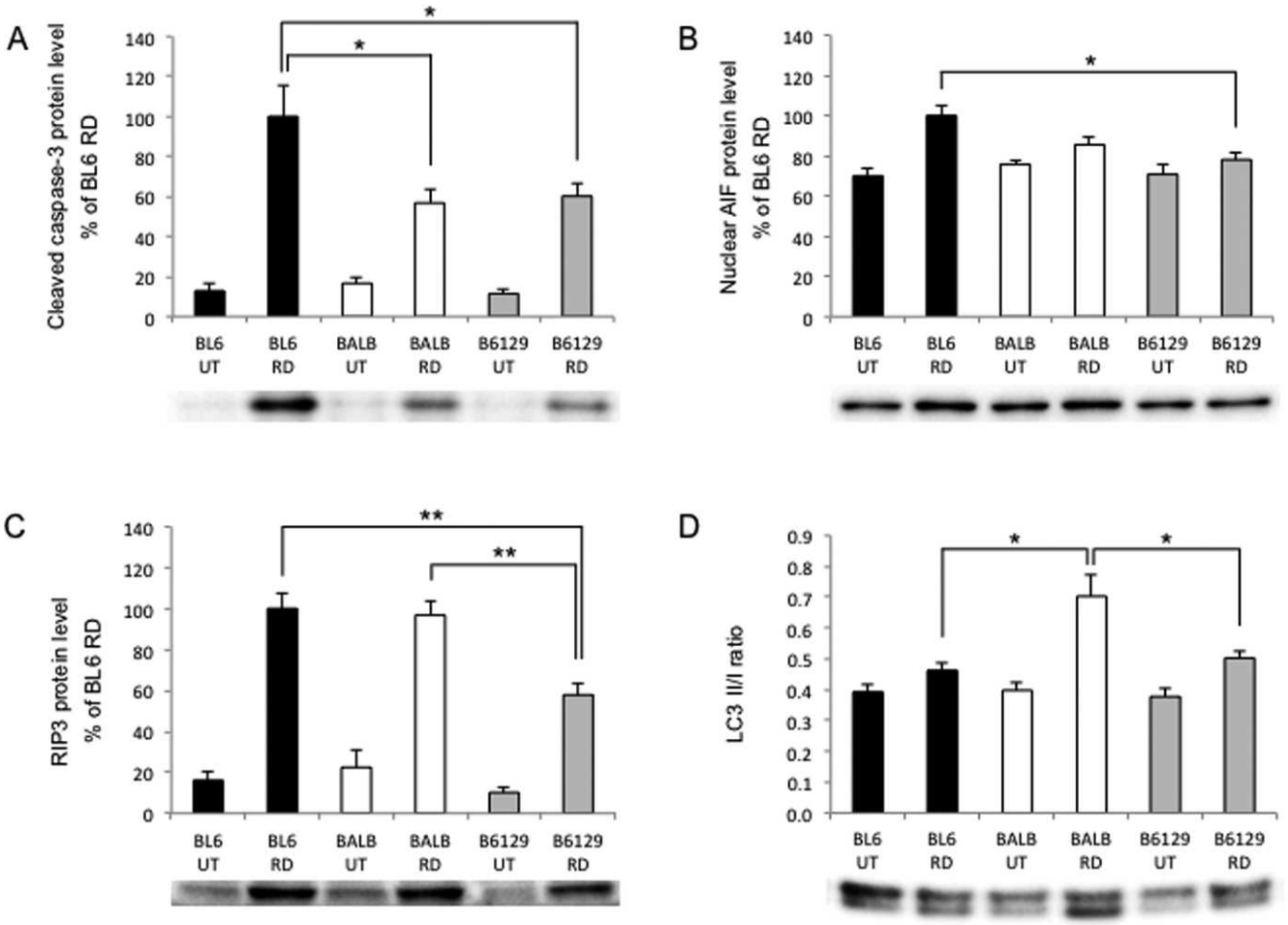

Figure 2. Difference in cell death signaling after RD. (**A–D**) Western blot analysis at 24 hours after RD ($n = 6$ each). (**A**) Cleaved caspase-3 was significantly higher in C57BL/6 than BALB/c and B6129SF2 (*$P < 0.05$ each). (**B**) Nuclear AIF was significantly higher in C57BL/6 than B6129SF2 (*$P < 0.05$). (**C**) RIP3 was significantly higher in C57BL/6 and BALB/c than B6129SF2 (**$P < 0.01$ each). (**D**) LC3 II/I ratio was significantly higher in BALB/c than C57BL/6 and B6129SF2 (*$P < 0.05$ each). (**A–C**) The *bar graphs* indicate the relative level of cleaved caspase-3, nuclear AIF, or RIP3 to β-actin or TBP by densitometric analysis. (**A–D**) Each sample for Western blot analysis includes at least six retinas.

that NGF activates the PI3-kinase/Akt pathway through TrkA phosphorylation, which leads to survivin upregulation.[62,63] In this study, RD resulted in increased survivin levels in all three strains. However, the level of survivin generated by RD was significantly less in BALB/c (74%) compared with C57BL/6 (100%) and B6129SF2 (97%; *$P < 0.05$ each; Fig. 4B). These results are in accordance with phosphorylated TrkA levels in each strain.

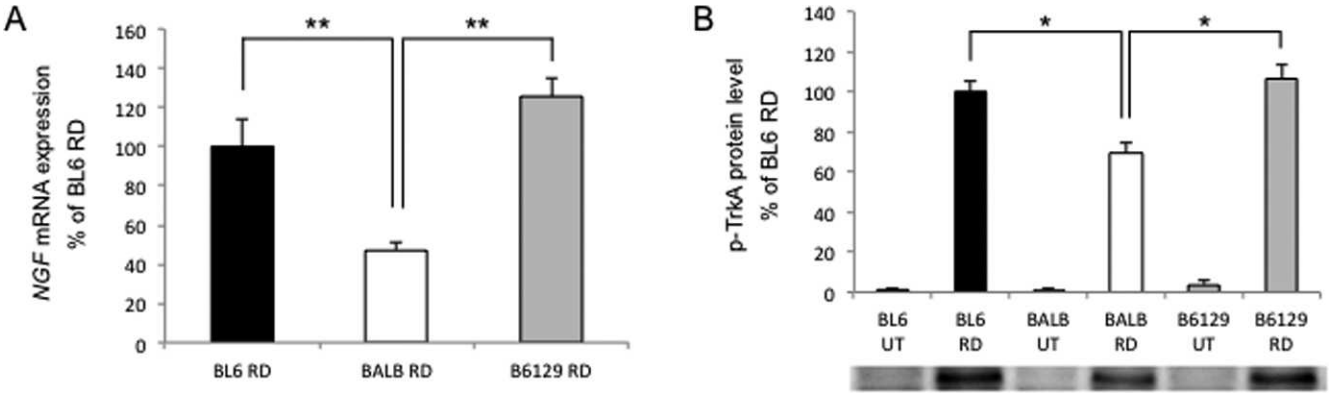

Figure 3. Difference in neurotrophin expression after RD. (**A**) Quantitative real-time PCR analysis for NGF in the retina at 24 hours after RD ($n = 6$ each). Mouse strain BALB/c showed significantly less *NGF* mRNA expression than C57BL/6 and B6129SF2 (**$P < 0.01$ each). (**B**) Western blot analysis for phosphorylated TrkA at 24 hours after RD ($n = 6$ each). Mouse strain BALB/c showed significantly less phosphorylated TrkA protein levels than C57BL/6 and B6129SF2 (*$P < 0.05$ each). The *bar graphs* indicate the relative level of phosphorylated TrkA to β-actin by densitometric analysis. Each sample for Western blot analysis includes at least six retinas.

Investigative Ophthalmology & Visual Science

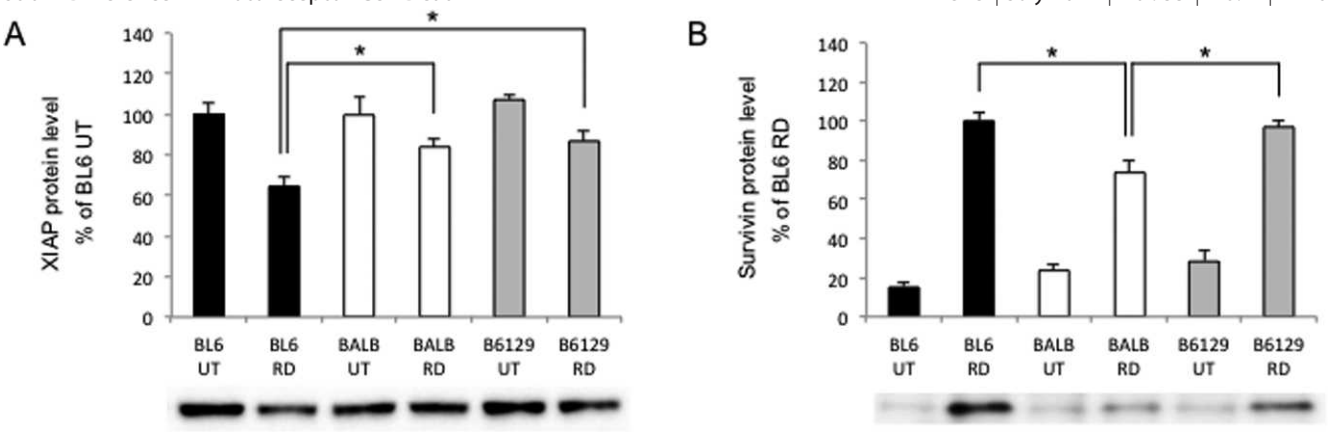

FIGURE 4. Difference in IAP protein levels after RD. (**A**, **B**) Western blot analysis at 24 hours after RD ($n = 6$ each). (**A**) X-linked IAP (XIAP) was significantly lower in C57BL/6 than BALB/c and B6129SF2 ($^*P < 0.05$ each). (**B**) Survivin was significantly less in BALB/c than C57BL/6 and B6129SF2 ($^*P < 0.05$ each). The *bar graphs* indicate the relative level of XIAP or survivin to β-actin by densitometric analysis. Each sample includes at least six retinas.

Strain Difference in Inflammatory Response After RD

We previously described that MCP-1 is an essential mediator of early infiltration of macrophage/microglia after RD.[18] Zacks et al.[19,23] reported that IL-6 expression was increased after RD using gene microarray analysis. Interleukin 6 is a pleiotropic cytokine with a role in inflammation as well as hematopoiesis, angiogenesis, cell differentiation, and neuronal survival.

In the current study, we evaluated MCP-1 and IL-6 protein levels by ELISA (Figs. 5A, 5B). Monocyte chemoattractant protein 1 was significantly higher in BALB/c (282 ± 45 pg/mg) than C57BL/6 (155 ± 14 pg/mg; $^*P < 0.05$) and B6129SF2 (129 ± 14 pg/mg; $^{**}P < 0.01$) at 24 hours after RD (Fig. 5A). Interleukin 6 was the highest in BALB/c (34.0 ± 4.2 pg/mg), followed in order by C57BL/6 (25.5 ± 4.5 pg/mg) and B6129SF2 (17.7 ± 1.4 pg/mg) at 24 hours after RD ($^*P < 0.05$ for BALB/c versus B6129SF2; Fig. 5B). After day 1, both MCP-1 and IL-6 levels were rapidly decreased in all strains (data not shown).

We next analyzed the inflammatory reaction by immunofluorescence detection of the macrophage/microglial marker CD11b (Figs. 5C, 5D). At 24 hours after RD, infiltration of CD11b-positive cells was significantly higher in BALB/c (129 ± 16 cells/mm^2) and C57BL/6 (157 ± 15 cells/mm^2) than B6129SF2 (72 ± 6 cells/mm^2; $^{**}P < 0.01$ each), while it was same level in all strains at 12 hours after RD. After day 1, CD11b-positive cell density in B6129SF2 was increased to the same level as the other two strains.

Glial fibrillary acidic protein (GFAP) is an intermediate filament protein which increases in astrocytes as well as activated Müller cells after RD.[20,64–66] It has been reported that reactive retinal glial cells contribute to retinal damage induced by RD.[20] In the current study, we evaluated GFAP levels in the retina before and 24 hours after RD by immunostaining. Consistent with previous studies, GFAP immunoreactivity was markedly increased after RD in all three strains. The pattern of GFAP immunoreactivity was similar among the strains either before or after RD (Supplementary Fig. S3).

DISCUSSION

This study investigated the difference in photoreceptor cell death after RD among three different mouse strains (C57BL/6, BALB/c, and B6129SF2). Our mouse model of RD consistently showed the peak of photoreceptor cell death 24 hours after RD.[43] At 12 hours after RD, photoreceptor cell death was significantly higher in C57BL/6 than BALB/c and B6129SF2 ($^*P < 0.05$ each), whereas at 24 hours after RD it was the highest in BALB/c, followed in order by C57BL/6 and B6129SF2 ($^{**}P < 0.01$ each). The ONL/INL ratio at 7 days after RD was the highest in B6129SF2 and lowest in BALB/c ($^*P < 0.05$), indicating that the total amount of photoreceptor cell death 7 days after RD was significantly higher in BALB/c than B6129SF2.

We modified a previously reported method for creating RD and achieved reproducible RD model.[43] Previous studies reported that the peak of photoreceptor cell death after RD occurs at day 3[6,8,10,15]; however, it occurs at day 1 in our model. It has been reported that photoreceptor cell death increases with increasing height of RD.[5,67] Photoreceptor cell damage with higher RD may be more extensive compared with shallow RD because of reduced diffusion of oxygen and essential nutrients from the choriocapillaris.[7,16] Our RD model has an extremely bullous and persistent RD in 60% of the fundus, which appears to accelerate photoreceptor cell death in the detached retina more than other RD models. In our mouse RD model, 4 μL of sodium hyaluronate is injected into the subretinal space to create a RD, whereas 1 to 2 μL of sodium hyaluronate is used in other mouse RD models.[15,20]

In the current study, we examined the key cell death signaling mediators (caspase, AIF, RIP kinase, and LC3) among the three strains. Mouse strain B6129SF2 showed lower levels of cell death signaling markers, paralleling the overall less photoreceptor cell death in that strain. However, the levels of pro–cell-death signaling cannot explain all of our observations since it was not BALB/c, but rather C57BL/6 that showed the most cell death signaling in terms of activation of caspase 3 and AIF nuclear translocation despite the overall more cell death observed in BALB/c. Receptor interacting protein 3 elevation was similar in these two strains and higher than B6129SF2. This suggests that the interplay between cell death and survival is more complex and strain dependent; furthermore, other pathways such as autophagy are important in determining the overall cell death.

Significant cross talk between apoptosis and autophagy is reported to exist. Kunchithapautham and Rohrer[68] described the increased expression of LC3-II in 661W photoreceptor cells pretreated with the broad-spectrum caspase inhibitor, zVAD-fmk. Maiuri et al.[69] also reported that cell death in apoptosis-deficient mouse embryonic fibroblasts was mediated by autophagic mechanisms. Furthermore, using a rat RD model, Besirli et al.[26] demonstrated the activation of autophagy after RD, which was critical for regulating photoreceptor apopto-

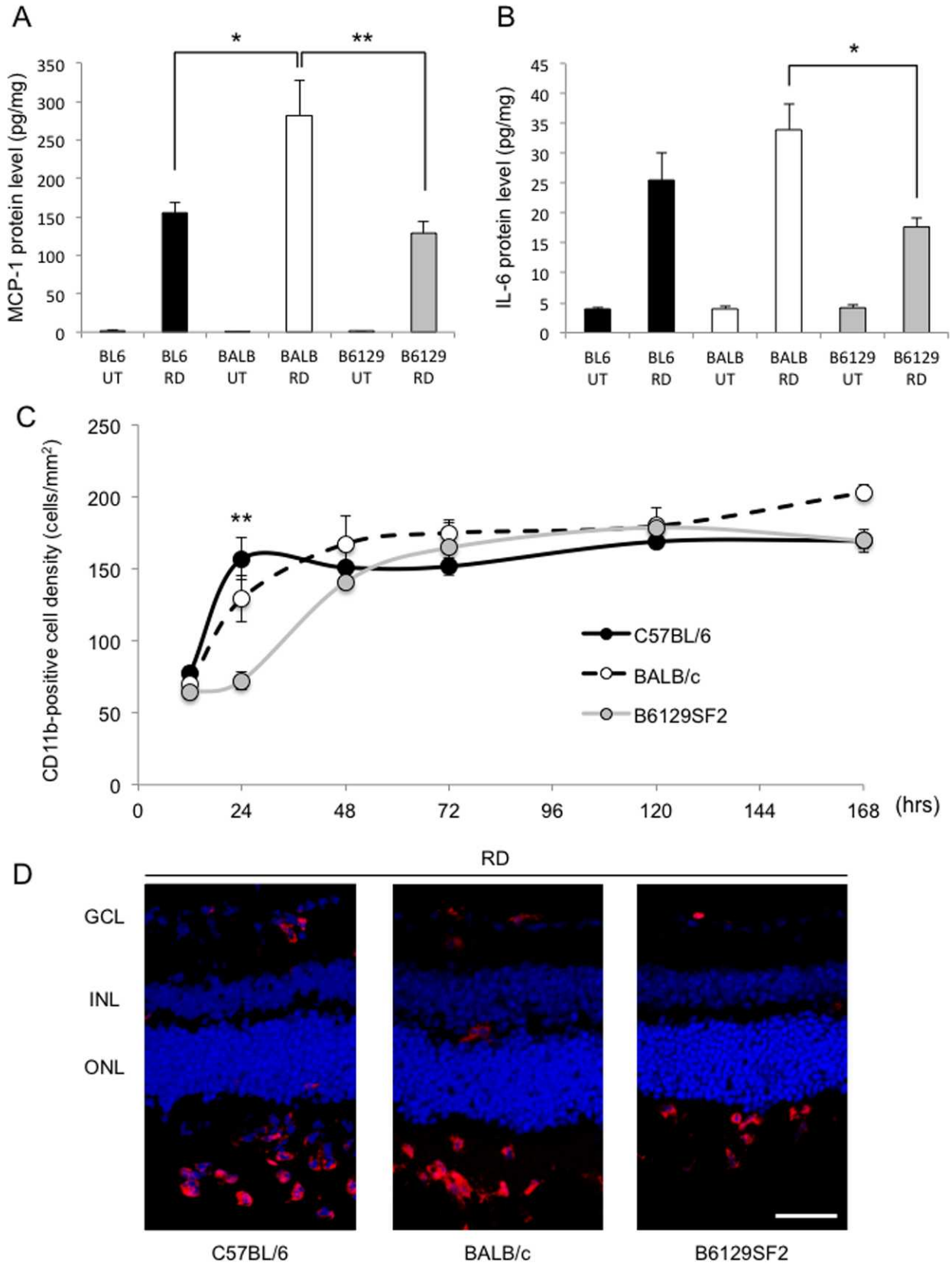

Figure 5. Difference in inflammatory response after RD. (**A**, **B**) ELISA to detect MCP-1 (**A**) and IL-6 (**B**) protein in the retina at 24 hours after RD ($n = 8$ each). Monocyte chemoattractant protein 1 was significantly higher in BALB/c than C57BL/6 ($^*P < 0.05$) and B6129SF2 ($^{**}P < 0.01$). Interleukin 6 was higher in BALB/c than B6129SF2 ($^*P < 0.05$). (**C**, **D**) Time course of CD11b-positive cell density ($n = 6$ each group and time point) (**C**) and CD11b (*red*) and TO-PRO-3 (*blue*) staining at 24 hours after RD (**D**). At 24 hours after RD, infiltration of CD11b-positive cells was significantly higher in BALB/c and C57BL/6 than B6129SF2 ($^{**}P < 0.01$ each), while it was same level in all strains at 12 hours after RD. After day 1, CD11b-positive cell density in B6129SF2 was increased to the same level to the other two strains. The graphs show mean ± SEM. *Scale bar*: 50 μm.

Investigative Ophthalmology & Visual Science

sis.[26] In the current study, BALB/c showed the highest LC3 II/I ratio but lower cleaved caspase-3 expression among the three strains at 24 hours after RD, suggesting that apoptosis signaling might be inhibited by the high level of autophagy signaling in BALB/c.

While autophagy can contribute to cell damage, it also may serve cell survival functions. Besirli et al.[26] reported that autophagy activation after RD reduced caspase activity, leading to the prevention of photoreceptor cell death. On the other hand, Kunchithapautham and Rohrer[68] demonstrated that DNA fragmentation and autophagy occurred in the same cells by TUNEL and membrane-associated LC3 staining using H_2O_2–treated 661W cells. Moreover, siRNAs targeting Atg5 and beclin1 (which are crucial for autophagy) prevented the cell death.[68] In our study, BALB/c showed the higher LC3 II/I ratio than C57BL/6 and B6129SF2 at 24 hours after RD. Thus, BALB/c might have more autophagic cell death than other two strains.

Since the cell death signals did not fully explain the difference in total photoreceptor cell death among the strains, we investigated changes in prosurvival pathways examining the expression of *NGF* mRNA and phosphorylation of its receptor TrkA as well as the downstream survivin at 24 hours after RD. These pathways were significantly repressed in BALB/c, which is consistent with the highest photoreceptor cell death at 24 hours after RD and the lowest ONL/INL ratio at 7 days after RD. Xiaodong and associates[57] reported that intravitreal injection of exogenous recombinant NGF could protect photoreceptor cell death in experimental rat RD. The mechanism by which NGF protects photoreceptor cells from degeneration is not clearly known; however, it has been suggested that NGF exerts its neuroprotective effect on photoreceptor cells in an indirect manner since TrkA has been reported to exist in Müller cells, astrocytes, the external part of INL, ganglion cells, and axons in the nerve fiber layer, but not in photoreceptor cells.[50–56] Accumulating results indicate that Müller cells might be important contributors to this mechanism.[70,71] Dubois-Dauphin et al.[72] demonstrated that loss of Müller cells leads to photoreceptor cell death using the transgenic mice, in which Müller cells die in the early postnatal phase.[72] Our results suggest that endogenous NGF might play a critical role in preventing photoreceptor cell death after RD, while the relationship between cell death and rescue signaling remains to be elucidated.

We previously reported that MCP-1 is an essential mediator of early infiltration of macrophage/microglia after RD, and that blockade of this pathway leads to enhanced photoreceptor survival.[18] In our current study, MCP-1 level was the highest in the strain with the most cell death and highest IL-6 levels (BALB/c), but was not different among C57BL/6 and B6129SF2 at 24 hours after RD. However, the infiltration of CD11b-positive cells at 24 hours did not parallel the different levels of MCP1 among the strains and C57BL/6 had almost similar kinetics to BALB/c despite lower levels of MCP1, whereas B6129SF2 who had MCP-1 levels equal to C57BL/6 had minimal infiltration at 24 hours. It is of interest that all three strains had similar CD1b infiltrate from day 2 onward. The governing of macrophage infiltration appears to be quite complex since the strain differences in the levels and kinetics of infiltration of the CD11b cells not only did not match perfectly with inflammatory cytokines (MCP-1 and IL-6), but also did not match with cell death as measured with TUNEL, suggesting more factors might govern their accumulation, function, and clearance. More studies are needed to investigate the subspecies of the infiltrating inflammatory cells after RD in order to better understand the interplay between inflammation and neural cell death/protection.

Our results showed significant differences among three mouse strains in the photoreceptor cell death, cell death signaling, neurotrophin expression, IAP protein levels, and inflammatory response after RD. Therefore, special attention needs to be paid to compare the data from different strains with RD. When using transgenic mice, it is essential to use the appropriate strain and age-matched controls. Moreover, these results suggest the presence of genetic factors that affect photoreceptor cell death after RD. Understanding the role of the genetic factors might provide new therapeutic targets for preventing photoreceptor cell death after RD.

Acknowledgments

We thank Wendy Chao for her support in critical review.

Supported by Foundation Lions Eye Research Fund (DGV); The Yeatts Family Foundation (DGV, JWM); a 2013 Macula Society Research Grant award (DGV); a Bausch & Lomb Vitreoretinal Fellowship (HM); a Special Scholar Award (KMC), a Physician Scientist Award (DGV), and a unrestricted grant (JWM) from the Research to Prevent Blindness Foundation; NIH R01EY022084–01/S1 (KMC); NEI R21EY023079-01A1 (DGV); and NEI Grant EY014104 (MEEI Core Grant). The content is solely the responsibility of the authors and does not necessarily represent the official views of the National Eye Institute or the National Institutes of Health.

Disclosure: **H. Matsumoto**, None; **K. Kataoka**, None; **P. Tsoka**, None; **K.M. Connor**, None; **J.W. Miller**, None; **D.G. Vavvas**, None

References

1. Mitry D, Fleck BW, Wright AF, Campbell H, Charteris DG. Pathogenesis of rhegmatogenous retinal detachment: predisposing anatomy and cell biology. *Retina*. 2010;30:1561–1572.
2. Dunaief JL, Dentchev T, Ying GS, Milam AH. The role of apoptosis in age-related macular degeneration. *Arch Ophthalmol*. 2002;120:1435–1442.
3. Barber AJ, Lieth E, Khin SA, Antonetti DA, Buchanan AG, Gardner TW. Neural apoptosis in the retina during experimental and human diabetes. Early onset and effect of insulin. *J Clin Invest*. 1998;102:783–791.
4. Hellstrom A, Smith LE, Dammann O. Retinopathy of prematurity. *Lancet*. 2013;382:1445–1457.
5. Machemer R. Experimental retinal detachment in the owl monkey. IV. The reattached retina. *Am J Ophthalmol*. 1968;66:1075–1091.
6. Cook B, Lewis GP, Fisher SK, Adler R. Apoptotic photoreceptor degeneration in experimental retinal detachment. *Invest Ophthalmol Vis Sci*. 1995;36:990–996.
7. Mervin K, Valter K, Maslim J, Lewis G, Fisher S, Stone J. Limiting photoreceptor death and deconstruction during experimental retinal detachment: the value of oxygen supplementation. *Am J Ophthalmol*. 1999;128:155–164.
8. Hisatomi T, Sakamoto T, Murata T, et al. Relocalization of apoptosis-inducing factor in photoreceptor apoptosis induced by retinal detachment in vivo. *Am J Pathol*. 2001;158:1271–1278.
9. Jacobs GH, Calderone JB, Sakai T, Lewis GP, Fisher SK. An animal model for studying cone function in retinal detachment. *Doc Ophthalmol*. 2002;104:119–132.
10. Hisatomi T, Sakamoto T, Goto Y, et al. Critical role of photoreceptor apoptosis in functional damage after retinal detachment. *Curr Eye Res*. 2002;24:161–172.
11. Lewis GP, Charteris DG, Sethi CS, Leitner WP, Linberg KA, Fisher SK. The ability of rapid retinal reattachment to stop or

reverse the cellular and molecular events initiated by detachment. *Invest Ophthalmol Vis Sci*. 2002;43:2412–2420.

12. Linberg KA, Sakai T, Lewis GP, Fisher SK. Experimental retinal detachment in the cone-dominant ground squirrel retina: morphology and basic immunocytochemistry. *Vis Neurosci*. 2002;19:603–619.
13. Sakai T, Calderone JB, Lewis GP, Linberg KA, Fisher SK, Jacobs GH. Cone photoreceptor recovery after experimental detachment and reattachment: an immunocytochemical, morphological, and electrophysiological study. *Invest Ophthalmol Vis Sci*. 2003;44:416–425.
14. Zacks DN, Hanninen V, Pantcheva M, Ezra E, Grosskreutz C, Miller JW. Caspase activation in an experimental model of retinal detachment. *Invest Ophthalmol Vis Sci*. 2003;44:1262–1267.
15. Yang L, Bula D, Arroyo JG, Chen DF. Preventing retinal detachment-associated photoreceptor cell loss in Bax-deficient mice. *Invest Ophthalmol Vis Sci*. 2004;45:648–654.
16. Lewis GP, Talaga KC, Linberg KA, Avery RL, Fisher SK. The efficacy of delayed oxygen therapy in the treatment of experimental retinal detachment. *Am J Ophthalmol*. 2004;137:1085–1095.
17. Zacks DN, Zheng QD, Han Y, Bakhru R, Miller JW. FAS-mediated apoptosis and its relation to intrinsic pathway activation in an experimental model of retinal detachment. *Invest Ophthalmol Vis Sci*. 2004;45:4563–4569.
18. Nakazawa T, Hisatomi T, Nakazawa C, et al. Monocyte chemoattractant protein 1 mediates retinal detachment-induced photoreceptor apoptosis. *Proc Natl Acad Sci U S A*. 2007;104:2425–2430.
19. Zacks DN, Han Y, Zeng Y, Swaroop A. Activation of signaling pathways and stress-response genes in an experimental model of retinal detachment. *Invest Ophthalmol Vis Sci*. 2006;47:1691–1695.
20. Nakazawa T, Takeda M, Lewis GP, et al. Attenuated glial reactions and photoreceptor degeneration after retinal detachment in mice deficient in glial fibrillary acidic protein and vimentin. *Invest Ophthalmol Vis Sci*. 2007;48:2760–2768.
21. Nakazawa T, Nakazawa C, Matsubara A, et al. Tumor necrosis factor-alpha mediates oligodendrocyte death and delayed retinal ganglion cell loss in a mouse model of glaucoma. *J Neurosci*. 2006;26:12633–12641.
22. Lewis GP, Chapin EA, Byun J, Luna G, Sherris D, Fisher SK. Muller cell reactivity and photoreceptor cell death are reduced after experimental retinal detachment using an inhibitor of the Akt/mTOR pathway. *Invest Ophthalmol Vis Sci*. 2009;50:4429–4435.
23. Zacks DN. Gene transcription profile of the detached retina (An AOS Thesis). *Trans Am Ophthalmol Soc*. 2009;107:343–382.
24. Besirli CG, Chinskey ND, Zheng QD, Zacks DN. Inhibition of retinal detachment-induced apoptosis in photoreceptors by a small peptide inhibitor of the Fas receptor. *Invest Ophthalmol Vis Sci*. 2010;51:2177–2184.
25. Trichonas G, Murakami Y, Thanos A, et al. Receptor interacting protein kinases mediate retinal detachment-induced photoreceptor necrosis and compensate for inhibition of apoptosis. *Proc Natl Acad Sci U S A*. 2010;107:21695–21700.
26. Besirli CG, Chinskey ND, Zheng QD, Zacks DN. Autophagy activation in the injured photoreceptor inhibits Fas-mediated apoptosis. *Invest Ophthalmol Vis Sci*. 2011;52:4193–4199.
27. Chinskey ND, Zheng QD, Zacks DN. Control of photoreceptor autophagy after retinal detachment: the switch from survival to death. *Invest Ophthalmol Vis Sci*. 2014;55:688–695.
28. Susin SA, Lorenzo HK, Zamzami N, et al. Molecular characterization of mitochondrial apoptosis-inducing factor. *Nature*. 1999;397:441–446.
29. Holler N, Zaru R, Micheau O, et al. Fas triggers an alternative, caspase-8-independent cell death pathway using the kinase RIP as effector molecule. *Nat Immunol*. 2000;1:489–495.
30. Festjens N, Vanden Berghe T, Vandenabeele P. Necrosis, a well-orchestrated form of cell demise: signalling cascades, important mediators and concomitant immune response. *Biochim Biophys Acta*. 2006;1757:1371–1387.
31. Golstein P, Kroemer G. Cell death by necrosis: towards a molecular definition. *Trends Biochem Sci*. 2007;32:37–43.
32. Degterev A, Hitomi J, Germscheid M, et al. Identification of RIP1 kinase as a specific cellular target of necrostatins. *Nat Chem Biol*. 2008;4:313–321.
33. Degterev A, Huang Z, Boyce M, et al. Chemical inhibitor of nonapoptotic cell death with therapeutic potential for ischemic brain injury. *Nat Chem Biol*. 2005;1:112–119.
34. Xie Z, Klionsky DJ. Autophagosome formation: core machinery and adaptations. *Nat Cell Biol*. 2007;9:1102–1109.
35. Ichimura Y, Kirisako T, Takao T, et al. A ubiquitin-like system mediates protein lipidation. *Nature*. 2000;408:488–492.
36. Friedman DS, Katz J, Bressler NM, Rahmani B, Tielsch JM. Racial differences in the prevalence of age-related macular degeneration: the Baltimore Eye Survey. *Ophthalmology*. 1999;106:1049–1055.
37. Quigley HA, Broman AT. The number of people with glaucoma worldwide in 2010 and 2020. *Br J Ophthalmol*. 2006;90:262–267.
38. Zouboulis CC. Epidemiology of Adamantiades-Behcet's disease. *Ann Med Interne (Paris)*. 1999;150:488–498.
39. LaVail MM, Gorrin GM, Repaci MA. Strain differences in sensitivity to light-induced photoreceptor degeneration in albino mice. *Curr Eye Res*. 1987;6:825–834.
40. Kipnis J, Yoles E, Schori H, Hauben E, Shaked I, Schwartz M. Neuronal survival after CNS insult is determined by a genetically encoded autoimmune response. *J Neurosci*. 2001;21:4564–4571.
41. Rohan RM, Fernandez A, Udagawa T, Yuan J, D'Amato RJ. Genetic heterogeneity of angiogenesis in mice. *FASEB J*. 2000;14:871–876.
42. Nakao S, Maruyama K, Zandi S, et al. Lymphangiogenesis and angiogenesis: concurrence and/or dependence? Studies in inbred mouse strains. *FASEB J*. 2010;24:504–513.
43. Matsumoto H, Miller JW, Vavvas DG. Retinal detachment model in rodents by subretinal injection of sodium hyaluronate. *J Vis Exp*. 2013;79. doi:10.3791/50660.
44. Matsumoto H, Murakami Y, Kataoka K, et al. Mammalian STE20-like kinase 2, not kinase 1, mediates photoreceptor cell death during retinal detachment. *Cell Death Dis*. 2014;5:e1269.
45. Lorenzo HK, Susin SA, Penninger J, Kroemer G. Apoptosis inducing factor (AIF): a phylogenetically old, caspase-independent effector of cell death. *Cell Death Differ*. 1999;6:516–524.
46. Galluzzi L, Kepp O, Kroemer G. RIP kinases initiate programmed necrosis. *J Mol Cell Biol*. 2009;1:8–10.
47. Dong K, Zhu H, Song Z, et al. Necrostatin-1 protects photoreceptors from cell death and improves functional outcome after experimental retinal detachment. *Am J Pathol*. 2012;181:1634–1641.
48. Kabeya Y, Mizushima N, Ueno T, et al. LC3, a mammalian homologue of yeast Apg8p, is localized in autophagosome membranes after processing. *EMBO J*. 2000;19:5720–5728.
49. Levi-Montalcini R. The nerve growth factor 35 years later. *Science*. 1987;237:1154–1162.
50. Rickman DW, Brecha NC. Expression of the proto-oncogene, Trk, receptors in the developing rat retina. *Vis Neurosci*. 1995;12:215–222.

Investigative Ophthalmology & Visual Science

51. Hallbook F, Backstrom A, Kullander K, Ebendal T, Carri NG. Expression of neurotrophins and Trk receptors in the avian retina. *J Comp Neurol*. 1996;364:664–676.
52. Oku H, Ikeda T, Honma Y, et al. Gene expression of neurotrophins and their high-affinity Trk receptors in cultured human Muller cells. *Ophthalmic Res*. 2002;34:38–42.
53. Ruiz-Ederra J, Hitchcock PF, Vecino E. Two classes of astrocytes in the adult human and pig retina in terms of their expression of high affinity NGF receptor (TrkA). *Neurosci Lett*. 2003;337:127–130.
54. Garcia M, Forster V, Hicks D, Vecino E. In vivo expression of neurotrophins and neurotrophin receptors is conserved in adult porcine retina in vitro. *Invest Ophthalmol Vis Sci*. 2003; 44:4532–4541.
55. Carmignoto G, Comelli MC, Candeo P, et al. Expression of NGF receptor and NGF receptor mRNA in the developing and adult rat retina. *Exp Neurol*. 1991;111:302–311.
56. Ugolini G, Cremisi F, Maffei L. TrkA, TrkB and p75 mRNA expression is developmentally regulated in the rat retina. *Brain Res*. 1995;704:121–124.
57. Sun X, Xu X, Wang F, et al. Effects of nerve growth factor for retinal cell survival in experimental retinal detachment. *Curr Eye Res*. 2007;32:765–772.
58. Chao MV, Hempstead BL. p75 and Trk: a two-receptor system. *Trends Neurosci*. 1995;18:321–326.
59. Liston P, Fong WG, Korneluk RG. The inhibitors of apoptosis: there is more to life than Bcl2. *Oncogene*. 2003;22:8568–8580.
60. Zadro-Lamoureux LA, Zacks DN, Baker AN, Zheng QD, Hauswirth WW, Tsilfidis C. XIAP effects on retinal detachment-induced photoreceptor apoptosis [corrected]. *Invest Ophthalmol Vis Sci*. 2009;50:1448–1453.
61. Li F, Ambrosini G, Chu EY, et al. Control of apoptosis and mitotic spindle checkpoint by survivin. *Nature*. 1998;396: 580–584.
62. Kuruvilla R, Ye H, Ginty DD. Spatially and functionally distinct roles of the PI3-K effector pathway during NGF signaling in sympathetic neurons. *Neuron*. 2000;27:499–512.
63. Kim S, Kang J, Qiao J, Thomas RP, Evers BM, Chung DH. Phosphatidylinositol 3-kinase inhibition down-regulates survivin and facilitates TRAIL-mediated apoptosis in neuroblastomas. *J Pediatr Surg*. 2004;39:516–521.
64. Lewis GP, Fisher SK. Up-regulation of glial fibrillary acidic protein in response to retinal injury: its potential role in glial remodeling and a comparison to vimentin expression. *Int Rev Cytol*. 2003;230:263–290.
65. Verardo MR, Lewis GP, Takeda M, et al. Abnormal reactivity of Müller cells after retinal detachment in mice deficient in GFAP and vimentin. *Invest Ophthalmol Vis Sci*. 2008;49:3659–3665.
66. Luna G, Lewis GP, Banna CD, Skalli O, Fisher SK. Expression profiles of nestin and synemin in reactive astrocytes and Muller cells following retinal injury: a comparison with glial fibrillar acidic protein and vimentin. *Mol Vis*. 2010;16:2511–2523.
67. Ross W, Lavina A, Russell M, Maberley D. The correlation between height of macular detachment and visual outcome in macula-off retinal detachments of $<$ or $=$ 7 days' duration. *Ophthalmology*. 2005;112:1213–1217.
68. Kunchithapautham K, Rohrer B. Apoptosis and autophagy in photoreceptors exposed to oxidative stress. *Autophagy*. 2007; 3:433–441.
69. Maiuri MC, Zalckvar E, Kimchi A, Kroemer G. Self-eating and self-killing: crosstalk between autophagy and apoptosis. *Nat Rev Mol Cell Biol*. 2007;8:741–752.
70. Harada T, Harada C, Nakayama N, et al. Modification of glial-neuronal cell interactions prevents photoreceptor apoptosis during light-induced retinal degeneration. *Neuron*. 2000;26: 533–541.
71. Zack DJ. Neurotrophic rescue of photoreceptors: are Muller cells the mediators of survival? *Neuron*. 2000;26:285–286.
72. Dubois-Dauphin M, Poitry-Yamate C, de Bilbao F, Julliard AK, Jourdan F, Donati G. Early postnatal Muller cell death leads to retinal but not optic nerve degeneration in NSE-Hu-Bcl-2 transgenic mice. *Neuroscience*. 2000;95:9–21.

Investigative Ophthalmology & Visual Science